Biomed. Mater. **7** (2012) 035004 (10pp) doi:10.1088/1748-6041/7/3/035004

Fibronectin adsorption and cell response on electroactive poly(vinylidene fluoride) films

C Ribeiro[1], J A Panadero[1], V Sencadas[1], S Lanceros-Méndez[1], M N Tamaño[2], D Moratal[2], M Salmerón-Sánchez[2,3,4] and J L Gómez Ribelles[2,3,4]

[1] Center/Departament of Physics, University of Minho, Campus de Gualtar, 4710-057 Braga, Portugal
[2] Center for Biomaterials and Tissue Engineering, Universidad Politécnica de Valencia, Camino de Vera s/n, 46022 Valencia, Spain
[3] Prince Felipe Research Center, Autopista del Saler 16, 46013 Valencia, Spain
[4] Networking Research Center on Bioengineering, Biomaterials and Nanomedicine (CIBER-BBN), Valencia, Spain

E-mail: lanceros@fisica.uminho.pt

Received 13 November 2011
Accepted for publication 25 January 2012
Published 23 February 2012
Online at stacks.iop.org/BMM/7/035004

Abstract
Due to the large potential of electroactive materials in novel tissue engineering strategies, the aim of this work is to determine if the crystalline phase and/or the surface electrical charge of electroactive poly(vinylidene fluoride), PVDF, have influence on the biological response in monolayer cell culture. Non-polar α-PVDF and electroactive β-PVDF were prepared. The β-PVDF films were poled by corona discharge to show negative or positive electrical surface charge density. It has been concluded that hydrophilicity of the PVDF substrates depends significantly on crystalline phase and polarity. Furthermore, by means of atomic force microscopy and an enzyme-linked immunosorbent assay test, it has been shown that positive or negative poling strongly influences the behavior of β-PVDF supports with respect to fibronectin (FN) adsorption, varying the exhibition of adhesion ligands of adsorbed FN. Culture of MC3T3-E1 pre-osteoeblasts proved that cell proliferation depends on surface polarity as well. These results open the viability of cell culture stimulation by mechanical deformation of a piezoelectric substrate that results in varying electrical charge densities on the substrate surface.

(Some figures may appear in colour only in the online journal)

1. Introduction

In the last decades, a wide variety of biomaterials with different properties have been studied and developed for biomedical applications. The cell/biomaterial interaction is a complex multi-step process that consists of several events. The first observable event *in vivo* or in a culture medium *in vitro* is the adsorption of proteins [1, 2]. Then, cell adhesion is mediated by cell-surface receptors that interact with specific ligands recognized in the layer of proteins previously adsorbed on the biomaterial surface [3, 4]. This protein layer is then reorganized and substituted by matrix proteins produced by the cells [5–7]. The quality of this first phase of cell/biomaterial interactions will influence the ability of the cells for proliferation and differentiation [8, 9].

The adsorption of matrix proteins such as fibronectin (FN) on substrate surfaces has been shown to be of large importance when culturing a variety of cells *in vitro* [10, 11]. The activity of adsorbed proteins (i.e. the distribution, concentration, conformation and motility) plays an important role in the biofunctionality of the biomaterial and allows understanding the biological response in cell culture in the laboratory

[4, 10]. The surface characteristics such as chemical composition, topography, viscoelastic properties, electric charge distribution and others determine how biological molecules will be absorbed by the surface and, more particularly, it also determines the conformation of adsorbed molecules [8, 12]. In this way, the behavior of cells cultured on substrates is highly dependent on these characteristics.

Previous studies have shown that electrically charged surfaces can influence cell behavior in different aspects such as growth, adhesion or morphology of cells. Beyond this, an electrically charged base for tissue engineering applications can be an interesting and promising approach [13]. Electroactive polymers, in particular piezoelectric poly(vinylidenefluoride) (PVDF), have attracted interest for biomedical applications in the fabrication of sensors and actuators and supports for cell culture. PVDF shows good biocompatibility, chemical resistance and, in particular, excellent electroactive properties, such as piezo-, pyro- and ferroelectricity [14]. This polymer can be obtained in four different crystalline phases, known as α, β, γ and δ, depending on the processing conditions. The β-phase is the one with the best piezoelectric and pyroelectric properties [14, 15].

The processing conditions optimizing the electroactive properties of β-PVDF have been previously studied both for films obtained from solvent evaporation [16, 17] and for films obtained by mechanical stretching [18, 19]. Particularly relevant for this work are previous studies by scanning force microscopy in a piezoresponse mode on the variations in the topological morphology and piezoelectric surface response of PVDF [20]. The piezoelectric activity at a mesoscale reflects the semicrystalline nature of the polymer: the piezoelectric activity of the β-phase at a mesoscopic scale is formed by dispersed nanoregions instead of classical domains. Clear differences in the poled region distribution and size, as well as in the local piezoactivity, have been identified in the different forms of PVDF: in the poled β-PVDF samples, the piezoelectric activity is more evident than before poling, with the piezoelectric activity of β-PVDF being independent of the processing method and morphology. No local piezoelectric activity is obtained in α-PVDF, corresponding to the nonpolarity of the macromolecule and the absence of macroscopic piezoelectric response.

Due to the potential of electroactive materials in the biological and biomedical fields, as they respond to electrical and mechanical solicitations, the aim of this work is to understand the role of the crystalline phase and polarity (i.e. surface charge) of electroactive supports on the cell response. With this purpose, the polymer with the largest electroactive response, β-phase PVDF, is investigated. As a first step, FN from human plasma was adsorbed on the different PVDF films from solutions of varying protein concentration. The surface density of the adsorbed FN was quantified by the enzyme-linked immunosorbent assay (ELISA) technique and the protein distribution and conformation was observed by atomic force microscopy (AFM). Thereafter, the effect of the polymer phase (α or β) and surface polarization on pre-osteoeblasts morphology, viability and proliferation was studied.

2. Materials and methods

2.1. Preparation of polymer films

PVDF films with a thickness of around 30 μm were obtained by casting a 20% solution of PVDF (*Solef* 1010 from *Solvay*) in *N,N*-dimethyl formamide (DMF) on a glass slide, applying the procedure reported in [16, 18]. Briefly, a glass slide with the spread solution was kept inside an oven at a controlled temperature of 120 °C for 60 min in order to assure the removal of the solvent and the isothermal crystallization of PVDF. After evaporation of the solvent, the sample was melted at 220 °C for 10 min. Then, the samples were removed from the oven, cooled to room temperature and removed from the glass. The polymer obtained by this procedure is predominantly α-PVDF. These films were then uniaxially drawn in a tensile machine at a stretching velocity of $\sim$ 1 mm min^{-1} at a temperature of 80 °C and a draw ratio ($R = L_{\text{fnal}}/L_{\text{initial}}$) of 5. After this procedure, the β-phase content of the samples is maximized up to $\sim$85% [18, 19]. The α to β-phase transformation is accompanied by a morphological transition from a spherulitic microstructure typical of the α-PVDF to a microfibrillar microstructure [18].

The electrical poling of the β-PVDF films was performed by a corona discharge inside a homemade chamber, and the piezoelectric response (d_{33}) of the poled samples was analyzed with a wide range d_{33}-meter (model 8000, APC Int. Ltd). The obtained value of the piezoelectric d_{33} coefficient for the poled samples was ~ -32 pC N^{-1} [16].

For cell culturing, circular PVDF films with 11 mm diameter were cut from the prepared films and sterilized by immersing several times in 70% ethanol for 15 min. Before cell seeding, the samples were washed five times for 5 min in the phosphate buffered saline (PBS) solution.

The films used in this study were α-PVDF, non-poled β-PVDF, 'poled +' β-PVDF (cell culture on the positively charged side of the sample) and 'poled –' β-PVDF (cell culture on the negatively charged side of the sample).

2.2. Contact angle measurements

The contact angle measurements (sessile drop in static mode) were performed at room temperature in a Data Physics OCA 20 device using distilled water as test liquid. All the micrographs were taken at the same focal distance (20 cm) and the volume of the drops was 20 μl. The contact angles were determined after six repetitions for each sample by using image analysis software (Image J) taking into account the entire drop shape.

2.3. Fibronectin adsorption

FN distribution on the different substrates was observed by AFM. FN from human plasma (Sigma) was adsorbed on the different PVDF films (α-PVDF, non-poled β-PVDF, 'poled +' β-PVDF and 'poled –' β-PVDF) by immersing the material sheets in FN solutions with different concentrations (1, 2 and 5 μg mL^{-1}) in modified saline (0.4% NaCl) for 10 min. After protein adsorption, the samples were rinsed in saline solution to eliminate the non-adsorbed protein. After that, the samples

were dried by exposing their surface to a nitrogen flow for a few minutes. AFM experiments were performed in a tapping mode in air immediately after sample preparation, using a Multimode AFM equipped with NanoScope IIIa controller from Veeco (Manchester, UK), under ambient conditions. Si cantilevers with a constant force of 2.8 N m^{-1} and a resonance frequency of 75 kHz were used. All the samples were characterized using a set-point amplitude ratio of around 0.9. The NanoScope 5.30r2 software version was used for the simultaneous recording of the height, phase and amplitude magnitudes of the images.

FN conformation was characterized by ELISA using monoclonal antibodies directed to cell adhesion domains. FN was adsorbed on all samples from a solution of 5 μg mL^{-1} for 1 h at 37 °C. The same samples without FN were used as controls. After FN adsorption, the surfaces of PVDF films were washed a few times in Dulbecco's PBS solution (DPBS) to remove non-adsorbed protein. After the FN adsorption, the nonspecific binding sites of the PVDF surface were blocked with DPBS++/BSA 1% for 30 min at room temperature. Then, the samples were incubated in the presence of monoclonal antibody IgG1 (DSHB University of Iowa), directed against the synergic site, in the FN repeat III_9, in dilution 1:4000 for 1 h at 37 °C. Following the incubation, each substrate was washed a few times with DPBS++/Tween 20. After being rinsed, a secondary antibody, antimouse alkaline phosphatase (Jackson Immuno Research), in dilution 1:5000 was added to the PVDF substrates for 1 h at 37 °C and then washed again as described above. The 4-methylumbelliferyl phosphate (4MUP; Sigma) was added to the samples for 45 min at 37 °C. The optical density (absorbance) of the wells at a wavelength of 465 nm was measured using a standard plate reader (Victor III, Perkin Elmer). Each experiment was performed in triplicate.

2.4. Cell adhesion and overall morphology

MC3T3-E1 cells (Riken cell bank, Japan) were cultivated in Dulbecco's modified Eagle's medium (DMEM) of 1 g L^{-1} glucose (Gibco) containing 10% fetal bovine serum (FBS) (Fisher) and 1% penicillin/streptomycin (P/S) at 37 °C in a CO_2 incubator. To investigate the initial cell adhesion and overall cell morphology, osteoblast-like cells suspended in 400 μL of serum-free DMEM were seeded on the substrates (PVDF samples discs and control glass covers) in 24-well TC plates at a cell density of 1×10^4 cells/well. All samples (three repetitions per sample) were previously coated with FN (20 μg mL^{-1}) for 1 h at 37 °C. After 2 h of incubation, the cells were rinsed with DPBS and fixed with a 10% neutral buffered formalin solution (Sigma-Aldrich) (1 h at 4 °C). After that, the substrates were washed with DPBS, permeabilized with Triton X-100 (5 min at room temperature) and incubated with a monoclonal mouse antibody against vinculin (Sigma-Aldrich) (1:400 in 1% DPBS/BSA, at room temperature for 1 h in agitation). The samples were rinsed a few times with 0.5% DPBS/Tween 20. Thereafter, Alexa Fluor 633-conjugated rabbit anti-mouse secondary antibody (Invitrogen) (1:200 in 1% DPBS/BSA, at room temperature for 1 h in agitation) was added and, at the same time, Bodipy FL Phallacidin (Invitrogen) for actine cytoskeleton (10 μL per sample) was also added. At last, the substrates were washed with 0.5% DPBS/Tween 20 and mounted with Vectashield containing DAPI. Focal adhesions were visualized by immune-fluorescence staining of vinculin. Images of adhered cells were taken with a fluorescence microscope (Leica DM6000B). Cytoplasma observed by cytoskeleton images were processed and analyzed using in-house software developed under MATLAB R2009b (The MathWorks, Inc., Natick, MA, USA). The mean cell area was calculated for every sample.

To determine the area covered by each cell, the processing of the cytoplasm images consisted firstly in grayscaling and equalization. Afterward, the images were binarized using Otsu's method [21], and the existing gaps were filled using an erosion morphological operator followed by a dilation one, using both a diamond structuring element of size 3. The resulting image was size-filtered using an opening morphological operator to eliminate remaining isolated pixels. In this way, a binary image stating the cytoplasm coverage was obtained, allowing the calculation of the total area covered by the cells or the mean area covered by each cell.

2.5. Cell viability and proliferation

For the study of cell viability and proliferation, the cells were seeded in 24-well TC plates with PVDF films and glass covers used as control at a cell density of 10^4 cells/well for 3 and 7 days, and incubated at 37 °C in a 5% CO_2 incubator. All samples (three repetitions for each sample) were previously immersed in a 20 μg mL^{-1} FN solution for 1 h at 37 °C. After washing all samples with DPBS, cells were suspended in DMEM without serum and seeded in the samples for 2 h at 37 °C in a 5% CO_2 incubator. Finally, the medium was replaced with DMEM containing 10% FBS.

For the quantification of cell viability and proliferation, MTS (3-(4,5-dymethylthiazol-2-yl)-5-(3-carboxymethoxyphenyl)-2(4-sulfopheny)-2H tetrazolium) assay (CellTiter 96^{TM} Aqueous One Solution Cell Proliferation Assay, Promega) was carried out. In this assay, the samples were washed a few times with DPBS. Then, 600 μL of the MTS solution (prepared with DMEM-LG without FBS, in a relation 1:5) was added to the substrates, which was incubated for 3 h at 37 oC in a 5% CO_2 incubator. At the end of the incubation period, 100 μL of each sample was transferred (in triplicate) into a 96-well plate. Finally, the absorbance at 490 nm, representing the proportion of viable cells, was measured by an optical spectrometer (Victor III, Perkin Elmer).

For cell number quantification, after fixation with a formalin buffered solution, the cell-support constructs were mounted with Vectashield containing DAPI for fluorescence microscopy (Leica DM6000B). For cell counting, the previously described software was used. Cell nuclei images were firstly grayscaled and equalized, providing an output grayscale image with its intensity values evenly distributed throughout the intensity range. These new images were then binarized through Otsu's method and size-filtered using

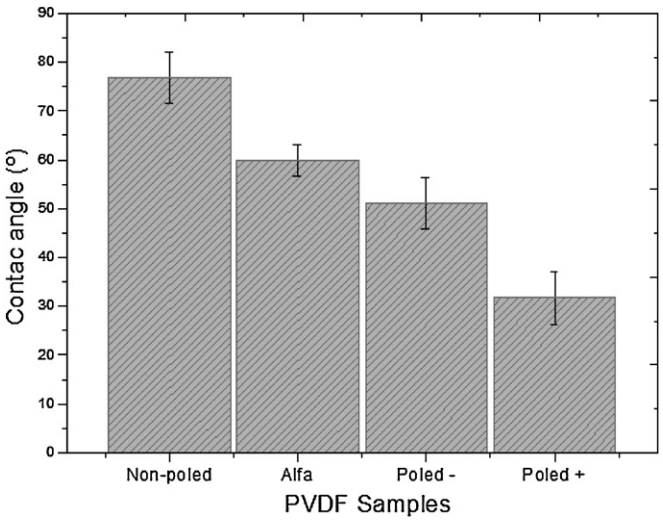

Figure 1. Evaluation of the water contact angle of different PVDF films (α, β non-poled, poled + and poled −).

an opening morphological operator. The cell nuclei were finally labeled and counted. Thus, cell number per mm^2 was calculated.

2.6. Statistical analysis

The results were expressed in mean ± standard deviation. Statistical comparisons were made by the analysis of variance (ANOVA) and F-tests were used for the evaluation of different groups. The differences were considered significant when $p < 0.05$.

3. Results

3.1. Contact angle measurements

Surface wettability (generally referred to as hydrophobicity/hydrophilicity) is one of the most important parameters affecting the biological response. According to the literature, wettability affects protein adsorption and cell adhesion [22, 23]. The wettability of the different PVDF film surfaces was determined showing that (figure 1) the non-poled β-PVDF film is more hydrophobic, with a contact angle of 76.8°, significantly higher than that measured in α-PVDF. Corona treatment produces an increase of the wettability of the β-PVDF films surface. The 'poled +' β-PVDF film is the most hydrophilic material with a contact angle of 31.8 °C, lower than that of the negatively charged surface.

3.2. Surface topography

The processing conditions of PVDF influence the phase content, morphology and electroactivity [20]. PVDF adopts an spherulitic morphology in the α-phase [15] that can be observed in the AFM pictures (figures 2(*a*), (*b*)). Crystal lamellae are apparent both in amplitude and phase images. The α-PVDF is a non-electroactive phase, and the mean roughness measured in 2 × 2 μm surface areas (average of three measurements) was around 68.5 nm. The topography of β-PVDF is quite different, being characterized by an oriented microfibrillar microstructure [18] (figures 2(*c*), (*d*)). When the β-PVDF sample is poled, there are no significant differences in morphology. With the AFM analysis of the local piezoresponse data of the non-poled β-PVDF and poled samples, it is shown [20] that a clear piezoresponse signal exists in both samples, being therefore the domain contrast more pronounced in the poled samples. The mean roughness of the non-poled β-PVDF is approximately 42 nm. The poling process does not affect the topography of the samples which maintain the same mean roughness [20]. The analysis of the line profiles of the topographic image and the corresponding domain contrast image confirms that there is no relationship between the surface piezoelectric response and the topography [20].

3.3. Protein adsorption

The distribution of FN adsorbed on the substrate can be observed by AFM provided the surface density of protein molecules is low enough. If the amount of protein adsorbed is too high, a continuous coating is formed preventing the observation of single protein molecules as well as their distribution at the material interface. This is the reason why FN was adsorbed on the substrates from aqueous solutions of varying concentration. Figure 3 shows AFM images (height, phase and amplitude) of non-poled β-PVDF films after FN adsorption from a 2 μg mL^{-1} solution.

Figure 4 shows the AFM images of the adsorbed proteins on the different PVDF films. FN distribution and organization of the surface depend significantly on the type of substrate and the concentration of the protein solutions.

The influence of the crystalline phase of the polymers is quite apparent when comparing α-PVDF and non-poled β-PVDF films. In both cases at the lower solution concentrations (1–2 μg mL^{-1}), homogeneously distributed FN molecules on the substrates are observed. When FN is adsorbed from a 2 μg mL^{-1} solution, a well-defined fibrillar distribution is found on β-PVDF, with the incipient formation of a protein network. On the other hand, a more homogeneous FN distribution is found on α-PVDF. Higher concentration of the FN solution (5 μg mL^{-1}) gives rise to the formation of a FN continuous protein coating that, in the case of α-PVDF, completely covers the spherulitic topography of the polymer. Likewise, α- and β-PVDF surfaces display similar appearance when they are completely covered by the protein layer.

In the poled β-PVDF films, the situation is quite different: a dense coating is formed already when FN is adsorbed from the 1 μg mL^{-1} solution. By increasing FN concentration, some changes in the topography of the protein surface are observed with no observable differences between the 'poled +' and 'poled –' β-PVDF substrates.

Single molecules could not be distinctly observed by AFM even in smaller scans areas. However, it can be inferred from FN adsorption from the solution of concentration 2 μg mL^{-1} that approximately the same amount of FN is adsorbed on the different surfaces. Furthermore, the differences in protein distribution observed at the lower concentrations suggest

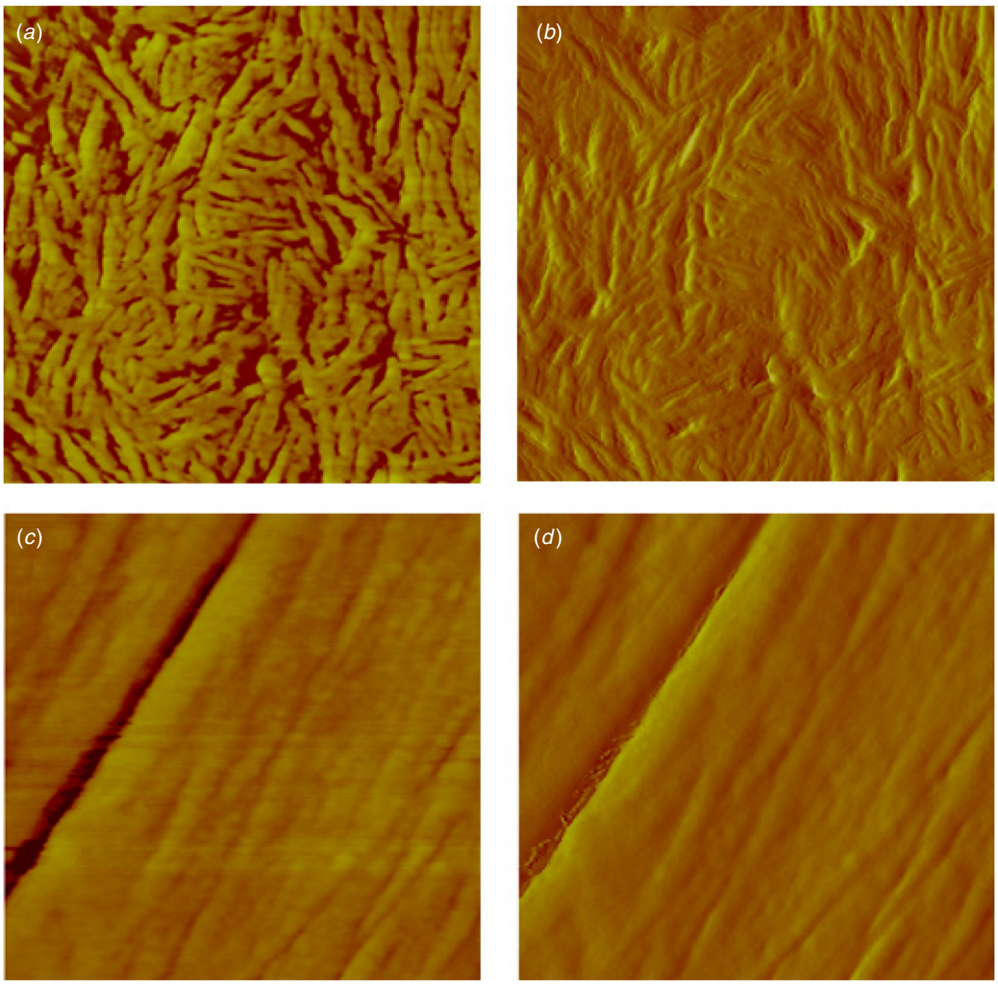

Figure 2. AFM images recorded in a 1 × 1 μm area of α-PVDF (*a*, *b*) and non-poled β-PVDF (*c*, *d*) surfaces. Phase (*a*, *c*) and amplitude (*b*, *d*) pictures are shown.

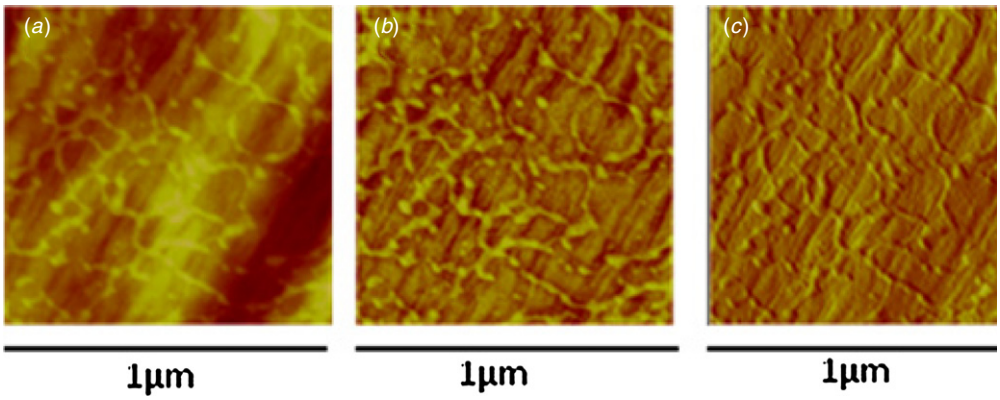

Figure 3. AFM images of non-poled β-PVDF with FN adsorbed form a solution with a concentration of 2 μg mL^{-1}. (*a*) Height, (*b*) phase and (*c*) amplitude magnitudes, respectively.

surface-induced changes in FN conformation [24]. Thus, an ELISA assay was performed to quantify differences in FN conformation using antibodies against adhesion-related domains, in order to obtain information about domain exposition. Figure 5 shows the results of the ELISA experiments for the different PVDF films and the control substrate. These results confirm that adhesion domains in poled β-PVDF films are more available for cell adhesion than in either non-poled β-PVDF or α-PVDF films. These domains are significantly masked in non-poled β-PVDF. Nevertheless, the difference between positively or negatively charged surfaces is not significant.

3.4. Cell attachment and cell proliferation

The overall morphology of the cells after 2 h is observed in figure 6. With respect to cell morphology and cell area, no significant differences were detected between poled and

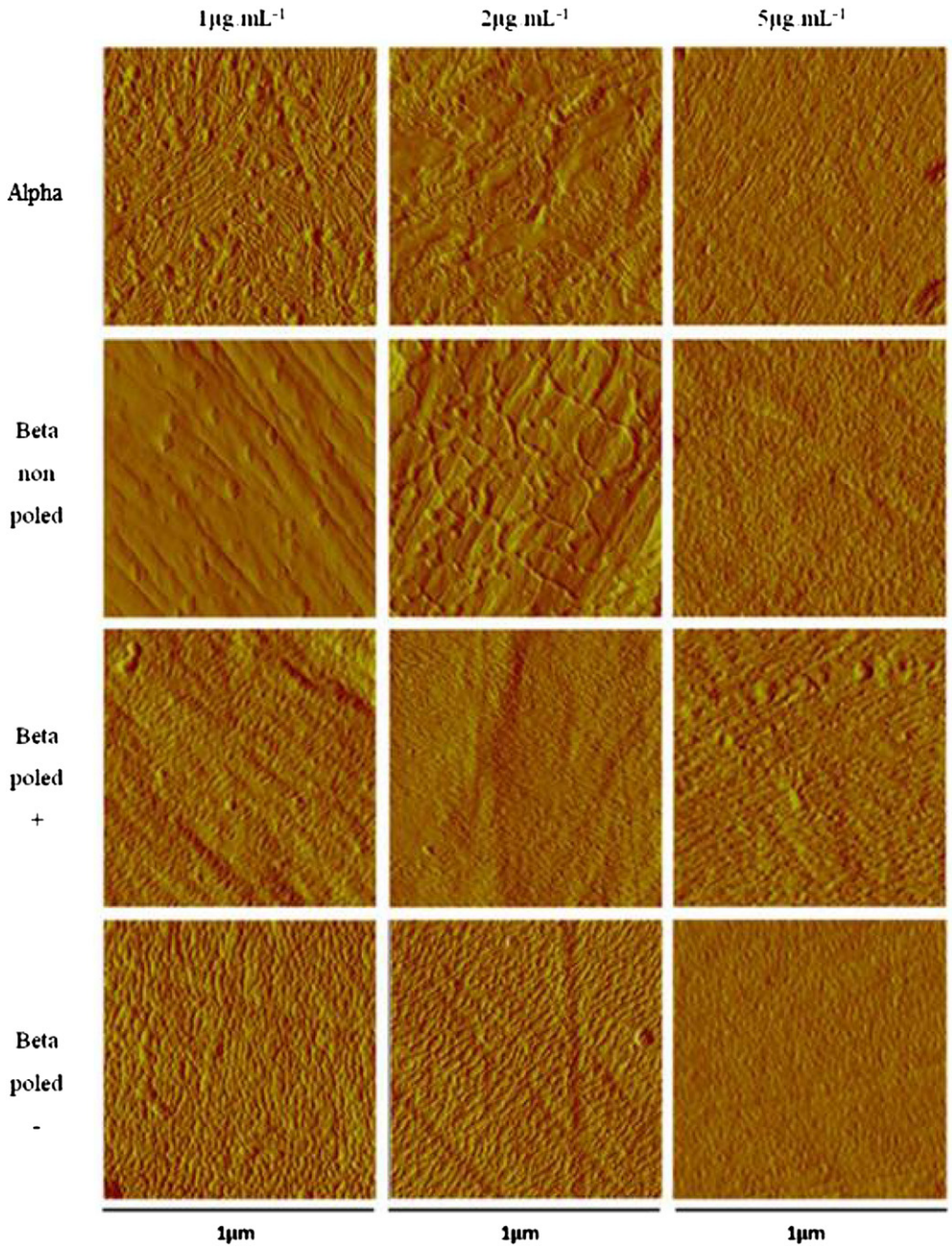

Figure 4. FN distribution as observed by the amplitude magnitude in AFM on the different substrates (α-PVDF, β-PVDF non-poled, 'poled +' β-PVDF and 'poled –' β-PVDF). FN was adsorbed for 10 min from solutions of different concentrations (1, 2 and 5 μg mL^{-1}).

non-poled films, as well as between films in different phases and the control glass.

Figure 7 shows the viability of the attached osteoblast cells in PVDF films and control after 3 and 7 days of culture. For all substrates, the number of viable cells increases with cell culture time. The substrates that seem to promote more active proliferation are α-PVDF and both positive and negative poled β-PVDF films, with no significant differences with respect to the control and among them. Cell viability is significantly lower in the case of non-poled PVDF as shown by the MTS test. Nevertheless, when cell nuclei are stained with DAPI and counted from fluorescence microscopy images, no significant differences in cell density between poled and non-poled β-PVDF substrates are found (figure 8).

The shapes of the cells attached on the different substrates are quite similar to each other and also similar to the control, as shown in figure 6. Cells are extended to the substrates and form well-defined and developed actin cytoskeleton. Using image analysis, the average surface covered by a cell was found to be 4475 $\pm$ 349 μm^2 with no significant differences among the substrates.

Cell density on the different substrates is represented in figure 8. After 3 days, all samples show a low number of cells. After 7 days of cell culture, the samples show significant differences in the number of cells. Moreover, it can also be

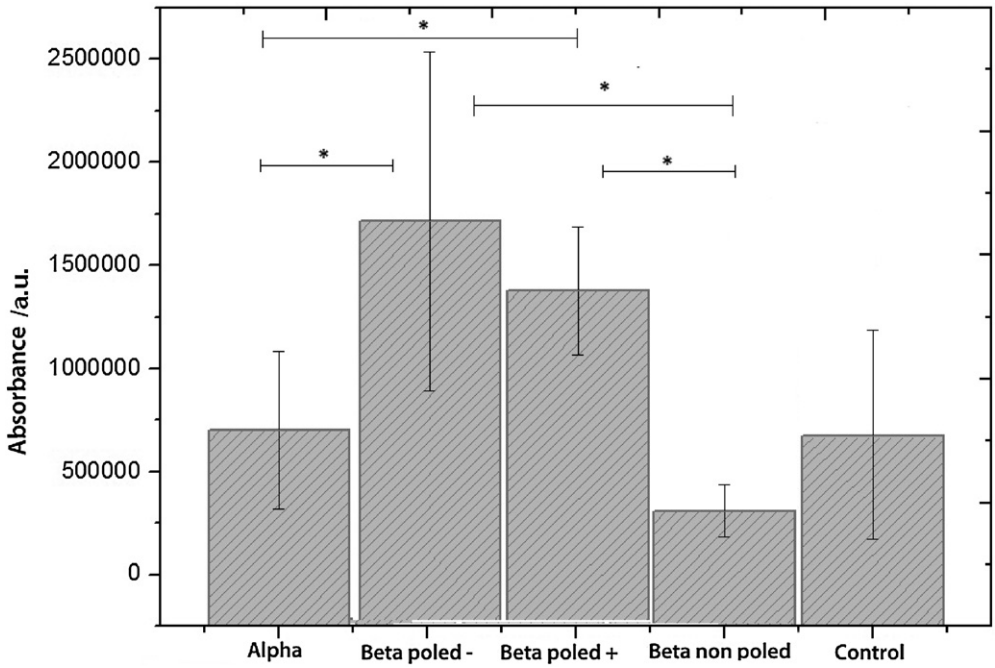

Figure 5. Monoclonal antibody binding for HFN7.One monoclonal antibody on the different PVDF samples after FN adsorption from a solution of concentration 5 μg mL^{-1}. * Significantly different ($p < 0.05$) PVDF samples.

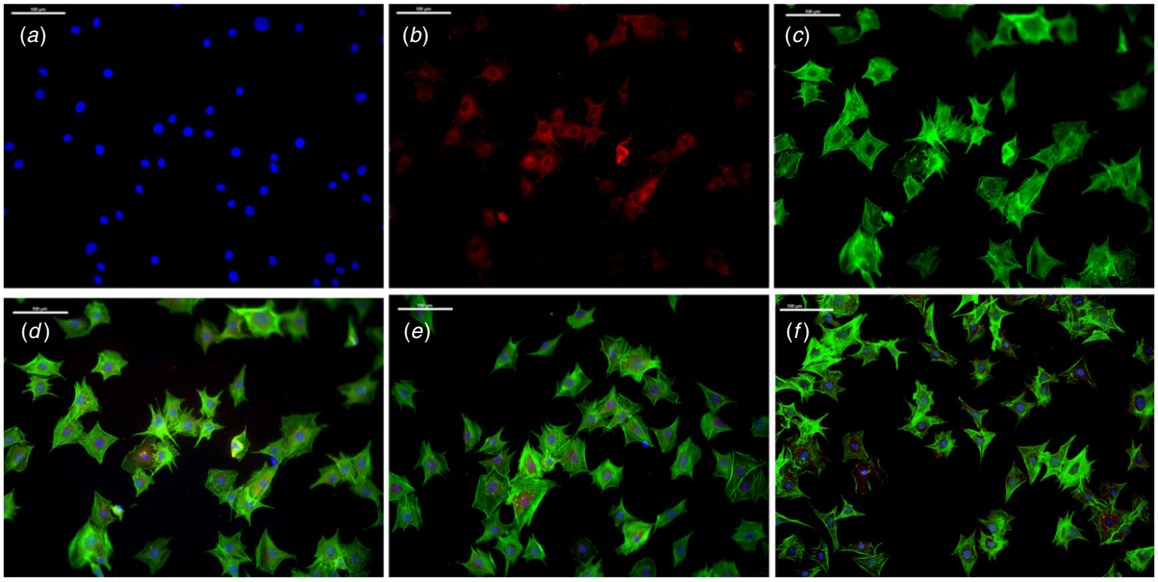

Figure 6. Cell culture with pre-osteoblast cells during 2 h in negative poled β-PVDF film (DAPI stained nuclei are shown in (*a*), vinculin expression in (*b*) and F-actin staining in (*c*), overlay (*d*)). For comparison the overlay images of α-PVDF film and control glass are shown in (*e*) and (*f*), respectively. The scale bar (100 μm) is valid for all the images.

observed that the cell distribution in the samples is not uniform. The control substrate shows the highest number of cells mm^{-2}, but comparing just the different PVDF films, the non-poled β-PVDF films show the lowest cell number and the poled α-PVDF films the highest number, with no significant differences with both positive and negative poled β-PVDF.

4. Discussion

The surface properties of PVDF are influenced by its crystalline phase, not only because of the different arrangement of crystal lamellae that, as shown in figure 2, leads to a different roughness and surface topography, but also due to a different surface energy leading to a quite hydrophobic material in the case of non-poled β-PVDF and to a more hydrophilic one in the case of α-PVDF. The reason for these differences is related to the different ordering of the permanent dipoles along the polymer chains in one and other crystalline orders. The configuration of PVDF chains crystallized in the α-phase is a non-polar trans-gauche-trans-gauche', TGTG', configuration, leading the consecutive permanent dipoles of the monomer units to orient in opposite directions, resulting in no net dipole

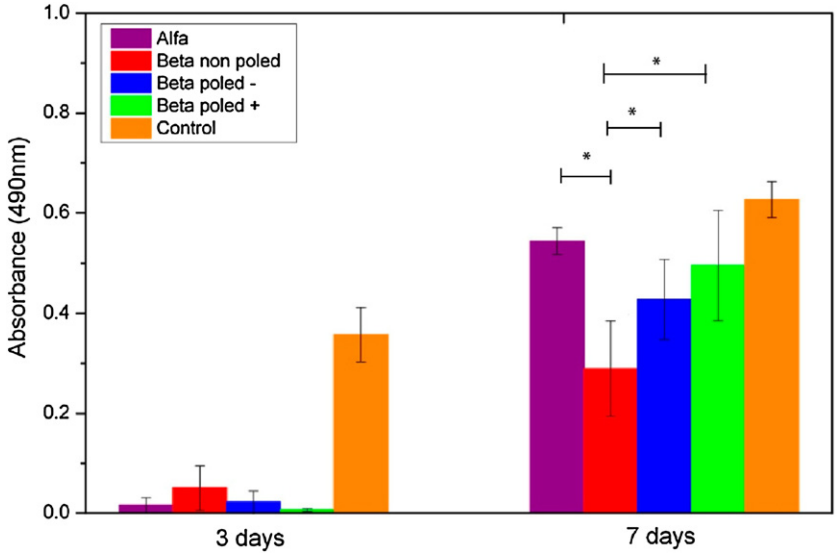

Figure 7. MTS absorbance results after cells seeded for 3 and 7 days on different PVDF films and the control substrate. * Significantly different ($p < 0.05$) PVDF samples.

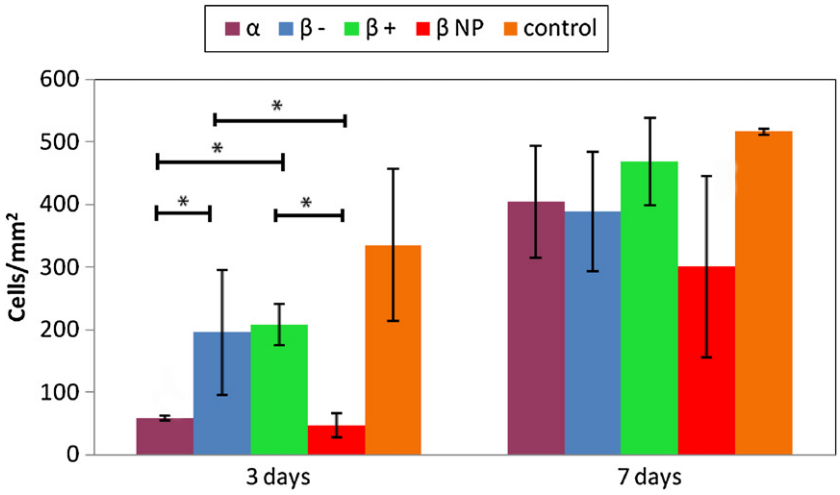

Figure 8. Cell density after for 3 and 7 days on different PVDF films and the control substrate. * Significantly different ($p < 0.05$) PVDF samples.

per unit cell [14, 25]. The crystalline β-phase has an all trans planar zigzag configuration, TTT, which confers the highest resulting permanent dipolar moment to this crystalline phase and consequently the best electroactive properties [14, 25]. Note, nevertheless, that the non-poled β-phase PVDF shows a random distribution of the dipolar moments, and therefore, the overall surface charge will be zero. Just by poling the samples, an alignment of the dipolar moments and an overall surface distribution will be achieved [20]

FN adsorption has been studied on different synthetic substrates. A straightforward correlation between substrate hydrophilicity and FN adsorption does not exist since other surface properties such as surface chemistry [26, 27], the presence of particular functional groups [28], roughness or the presence of patterning cues [27] also have an important effect on FN adsorption. While many studies have shown that a larger amount of protein get adsorbed on hydrophobic surfaces than on hydrophilic ones, as it is the case with other matrix proteins as laminin, fibrinogen or vitronectin [29, 30], the literature also shows many important examples of higher activity of FN on hydrophilic surfaces [31, 32]. On the other hand, the conformation of FN on the substrate is also highly influenced by other surface characteristics. It seems that an important characteristic of FN with respect to cell adhesion is its ability to intermolecular linkage forming a fibrillar structure (fibrillogenesis) or a protein network. Cell activity seems to be essential for fibrillogenesis but it has been observed in some synthetic substrates in absence of cells. This is the case of hydrophobous poly(ethyl acrylate) substrates [33, 34].

When the electroactive β-PVDF is poled by corona discharge, introducing a positive or negative electric charge density, the wettability of the surface increase significantly as shown in figure 1.

In the PVDF substrates of this work the observed behavior by adsorbed FN is peculiar in some aspects. Although the AFM images of figure 4 give no quantitative information about

protein adsorption, they suggest that adsorbed protein quantity is higher in poled β-PVDF than in non-poled β-PVDF or in α-PVDF but only when adsorbed from low FN concentration solutions. When FN is adsorbed from a 5 μg ml^{-1}, the FN layer observed in all samples looks similar. When dispersed protein domains are observed, the images suggest differences in distribution. The visual aspect in non-poled β-PVDF is clearly different than in α-PVDF when immersed in the same FN solution. Association in fibrils seems to appear only in non-poled β-PVDF, which can be related to the lower hydrophilicity of its surface. Randomly distributed FN aggregates can be observed in α-PVDF or in the poled samples at very low FN concentration.

Data from the ELISA experiments complement the information obtained from the AFM images. ELISA experiments were performed on samples after adsorption from a 5 μg mL^{-1} FN solution, in which the surface appearing in AFM is that of a homogeneous coating of the PVDF surface (figure 4). The exposition of cell adhesion domains is significantly higher in the poled β-PVDF samples with respect to non-poled samples and also with respect to the control. It seems that the presence of a surface distribution of electric charges overcomes the effect of other surface properties. On the one hand, exposition of adhesion ligands in poled samples is higher than that in non-poled β-PVDF, that shows the same topography, despite the latter having much lower wettability. In the same way, it is higher than in α-PVDF.

MC3T3-E1 pre-osteoblasts were seeded on the substrates previously coated with FN and in a culture medium in absence of serum in order to avoid the modification of the protein layer adsorbed on the substrate. In order to allow long-term culture, a medium with FBS was added after initial adhesion. Cells adhere to all the substrates develop focal adhesions and organize the actin cytoskeleton. The shape of the cells and the average surface covered per cell for the shortest times of cell culture seem to be equal in the four substrates under study. Some of the differences in MC3T3-E1 pre-osteoblasts are just shown after several days of culture and are in accordance with the differences shown in protein adsorption and conformation. The low absorbance in MTS experiments at 3 days culture does not allow us to detect significant differences among the different samples due to the small signal, the absorbance being much lower than in the control surface. Nevertheless, the cell numbers counted from fluorescence microscope images clearly show that cell numbers are higher in the poled β-PVDF samples that correlates with the availability of cell adhesion sequences of the adsorbed FN, as determined by ELISA tests. At 7 days culture, the cell number and MTS absorbance in the non-poled β-PVDF sample seem still to be smaller than those in the samples with a surface density of electric charges. MC3T3-E1 are highly proliferative cells, reaching confluence in few days in tissue culture polystyrene or in the glass slides used as controls in our experiments. This is shown by the high cell numbers and MTS signal after 3 days culture in the controls in contrast with the slower culture proliferation in all the PVDF substrates. Nevertheless, after relatively short times of culture cells reach confluence in all substrates, and at 7 days culture the cell numbers and MTS signal tend to be the same in the α- and positively or negatively poled β-PVDF samples and also nearly the same as that of the controls. Only non-poled β-PVDF shows significantly smaller MTS absorbance and small mean cell numbers than the rest culture surfaces at day 7. For longer culture time, this sample shows the same cell number than the others.

These experiments show that the presence of electrical charge on the surface of the piezoelectric material influences the distribution and conformation of adsorbed protein layers on the material surface and in turn on cell adhesion. In this sense, the difference between poled and non-poled states of the electroactive β-phase of PVDF is particularly significant. If this material is deformed by the action of mechanical forces, the piezoelectric effect will produce the variation of the electrical charge density at the interfaces with the biological tissue. Thus, this type of substrate can be used for simultaneous mechanical and electric stimulation of cells in culture.

5. Conclusions

It is shown that the polarization of a PVDF electroactive crystalline phase to create both negative and positive electrical charge surface densities modifies the conformation of adsorbed FN at the material surface and therefore cell adhesion on the FN-coated substrates. As a consequence, cell numbers on the substrate are significantly higher in poled than in non-poled samples. Differences in FN adsorption between α- and non-poled β-crystalline phases due to different surface topography, wettability and ordering of polymer chain groups are detectable but can be considered less important. In this way, these results open the possibility of developing active substrates for cell culture and tissue engineering, influencing cell response through the variation of the surface electrical charge density when a mechanical solicitation is applied.

Acknowledgments

This work is funded by FEDER funds through the 'Programa Operacional Factores de Competitividade—COMPETE' and by national funds by FCT—Fundação para a Ciência e a Tecnologia, project reference NANO/NMed-SD/0156/2007. CR thanks the INL for a PhD grant. VS and JAP thank the FCT for the SFRH/BPD/63148/2009 and SFRH/BD/64586/2009/grants, respectively. JLGR acknowledges the support of the Spanish Ministry of Education through project no MAT2010-21611-C03-01 (including the FEDER financial support), project EUI2008-00126 and funding in the Centro de Investigación Principe Felipe in the field of Regenerative Medicine through the collaboration agreement from the Conselleria de Sanidad (Generalitat Valenciana) and the Instituto de Salud Carlos III (Ministry of Science and Innovation). The authors thank Armando Ferreira for the help with the contact angle measurements and CENTI, Portugal, for allowing the use of the set-up.

References

[1] Ratner B D 2004 *Biomaterials Science: An Introduction to Materials in Medicine* (Amsterdam: Academic)

[2] Shard A G and Tomlins P E 2006 Biocompatibility and the efficacy of medical implants *Regen. Med.* **1** 789–800

[3] Klee D, Ademovic Z, Bosserhoff A, Hoecker H, Maziolis G and Erli H J 2003 Surface modification of poly(vinylidenefluoride) to improve the osteoblast adhesion *Biomaterials* **24** 3663–70

[4] Guerra N B *et al* 2010 Subtle variations in polymer chemistry modulate substrate stiffness and fibronectin activity *Soft Matter* **6** 4748–55

[5] Altankov G and Groth T 1994 Reorganization of substratum-bound fibronectin on hydrophilic and hydrophobic materials is related to biocompatibilityg *J. Mater. Sci., Mater. Med.* **5** 732–7

[6] Avnur Z and Geiger B 1981 The removal of extracellular fibronectin from areas of cell-substrate contact *Cell* **25** 121–32

[7] Altankov G, Groth T, Krasteva N, Albrecht W and Paul D 1997 Morphological evidence for a different fibronectin receptor organization and function during fibroblast adhesion on hydrophilic and hydrophobic glass substrata *J. Biomater. Sci. Polym. Ed.* **8** 721–40

[8] Anselme K 2000 Osteoblast adhesion on biomaterials *Biomaterials* **21** 667–81

[9] Wilson C J, Clegg R E, Leavesley D I and Pearcy M J 2005 Mediation of biomaterial-cell interactions by adsorbed proteins: a review *Tissue Eng.* **11** 1–18

[10] Whittle J D, Bullett N A, Short R D, Douglas C W I, Hollander A P and Davies J 2002 Adsorption of vitronectin, collagen and immunoglobulin-G to plasma polymer surfaces by enzyme linked immunosorbent assay (ELISA) *J. Mater. Chem.* **12** 2726–32

[11] Barrias C C, Martins M C L, Almeida-Porada G, Barbosa M A and Granja P L 2009 The correlation between the adsorption of adhesive proteins and cell behaviour on hydroxyl-methyl mixed self-assembled monolayers *Biomaterials* **30** 307–16

[12] Okada S, Ito H, Nagai A, Komotori J and Imai H 2010 Adhesion of osteoblast-like cells on nanostructured hydroxyapatite *Acta Biomater.* **6** 591–7

[13] Weber N, Lee Y S, Shanmugasundaram S, Jaffe M and Arinzeh T L 2010 Characterization and *in vitro* cytocompatibility of piezoelectric electrospun scaffolds *Acta Biomater.* **6** 3550–6

[14] Lovinger A J 1982 *Developments in Crystalline Polymers* (London: Elsevier)

[15] Nalwa H S 1995 *Ferroelectric Polymers: Chemistry, Physics and Applications* (New York: Marcel Dekker)

[16] Branciforti M C, Sencadas V, Lanceros-Mendez S and Gregorio R 2007 New technique of processing highly oriented poly(vinylidene fluoride) films exclusively in the beta phase *J. Polym. Sci.* B **45** 2793–801

[17] Sencadas V, Gregorio Filho R and Lanceros-Mendez S 2006 Processing and characterization of a novel nonporous poly(vinilidene fluoride) films in the [beta] phase *J. Non-Cryst. Solids* **352** 2226–9

[18] Sencadas V, Gregorio R and Lanceros-Mendez S 2009 Alpha to beta phase transformation and microestructural changes of PVDF films induced by uniaxial stretch *J. Macromol. Sci.-Phys.* B **48** 514–25

[19] Gomes J *et al* 2010 Influence of the β-phase content and degree of crystallinity on the piezo-and ferroelectric properties of poly(vinylidene fluoride) *Smart Mater. Struct.* **19** 065010

[20] Nunes J S, Wu A, Gomes J, Sencadas V, Vilarinho P M and Lanceros-Mendez S 2009 Relationship between the microstructure and the microscopic piezoelectric response of the alpha- and beta-phases of poly(vinylidene fluoride) *Appl. Phys* A **95** 875–80

[21] Otsu N 1979 Threshold selectino method from gray-level histograms *IEEE Trans. Syst. Man Cybern.* **9** 62–6

[22] Sigal G B, Mrksich M and Whitesides G M 1998 Effect of surface wettability on the adsorption of proteins and detergents *J. Am. Chem. Soc.* **120** 3464–73

[23] Vanwachem P B, Beugeling T, Feijen J, Bantjes A, Detmers J P and Vanaken W G 1985 Interaction of cultured human-endothelial cells with polymeric surfaces of different wettabilities *Biomaterials* **6** 403–8

[24] Hernandez J C R, Sanchez M S, Soria J M, Ribelles J L G and Pradas M M 2007 Substrate chemistry-dependent conformations of single laminin molecules on polymer surfaces are revealed by the phase signal of atomic force microscopy *Biophys. J.* **93** 202–7

[25] Bar-Cohen Y 2004 *Electroactive Polymer (EAP) Actuators as Artificial Muscles - Reality Potential and Challenges* 2nd edn (Bellingham, WA: SPIE) pp 89–120

[26] Roach P, Eglin D, Rohde K and Perry C 2007 Modern biomaterials: a review—bulk properties and implications of surface modifications *J. Mater. Sci., Mater. Med.* **18** 1263–77

[27] Tsapikouni T S and Missirlis Y F 2008 Protein–material interactions: from micro-to-nano scale *Mater. Sci. Eng.* B **152** 2–7

[28] Michael K E, Vernekar V N, Keselowsky B G, Meredith J C, Latour R A and García A J 2003 Adsorption-induced conformational changes in fibronectin due to interactions with well-defined surface chemistries *Langmuir* **19** 8033–40

[29] Schmidt D R, Waldeck H and Kao W J 2009 *Protein Adsorption to Biomaterials Biological Interactions on Materials Surfaces* ed D A Puleo and R Bizios (New York: Springer) pp 1–18

[30] Comelles J, Estévez M, Martínez E and Samitier J 2010 The role of surface energy of technical polymers in serum protein adsorption and MG-63 cells adhesion *Nanomedicine* **6** 44–51

[31] Garcia A J, Vega M D and Boettiger D 1999 Modulation of cell proliferation and differentiation through substrate-dependent changes in fibronectin conformation *Mol. Biol. Cell* **10** 785–98

[32] Llopis-Hernandez V, Rico P, Ballester-Beltran J, Moratal D and Salmeron-Sanchez M 2011 Role of surface chemistry in protein remodeling at the cell-material interface *PLoS One* **6**

[33] Salmeron-Sanchez M, Rico P, Moratal D, Lee T T, Schwarzbauer J E and Garcia A J 2011 Role of material-driven fibronectin fibrillogenesis in cell differentiation *Biomaterials* **32** 2099–105

[34] Gugutkov D, Gonzalez-Garcia C, Hernandez J C R, Altankov G and Salmeron-Sanchez M 2009 Biological activity of the substrate-induced fibronectin network: insight into the third dimension through electrospun fibers *Langmuir* **25** 10893–900